



Heterogeneous *para*-phenylamino sulfonic acid ligand functionalized on MCM-41 derived from rice husk ash: Selective mono-alkylated products of *tert*-butylation of phenol



Farook Adam*, Chien-Wen Kueh

School of Chemical Sciences, University Sains Malaysia, 11800 Penang, Malaysia

ARTICLE INFO

Article history:

Received 13 June 2014

Received in revised form

21 September 2014

Accepted 28 September 2014

Available online 7 October 2014

Keywords:

Organic-inorganic hybrid

MCM-41

Immobilization

tert-Butylation of phenol.

ABSTRACT

A new organo-inorganic hybrid material was prepared by immobilizing 3-(4-aminophenylamino)propane-1-sulfonic acid onto functionalized mesoporous MCM-41 via simple post-synthesis method. The hybrid organo MCM-41 preserved its hexagonal honey-comb configuration after both surface chemical modification and immobilization of sulfonic acid ligand. XRD analysis exhibited three well-resolved diffraction peaks corresponding to the highly ordered mesostructure. The five intense carbon peaks of solid-state CP-MAS ^{13}C NMR spectroscopy confirmed the grafting of sulfonic acid ligand onto the well-structured MCM-41. Surface properties of the material revealed a pore size of 1.98 nm and surface area of $468 \text{ m}^2 \text{ g}^{-1}$. The catalytic performance of this hybrid material was tested in the alkylation of phenol with *tert*-butanol (TBA) and showed a high catalytic activity leading to 99.5% conversion of *tert*-butyl alcohol and high selectivity to monoalkylated products.

© 2014 Elsevier B.V. All rights reserved.

1. Introduction

Alkylation of phenol with tertiary butyl alcohol is a typical Friedel-Crafts reaction that is important in industry due to the wide application of butylated products. 2-*tert*-Butylphenol (2-TBP) is an intermediate for fragrances and pesticides, whereas 4-*tert*-butylphenol (4-TBP) is used to make oils and phosphate esters [1]. The other commercial uses of butylated phenols include the essential feedstock for antioxidants, phenolic resins, ultraviolet absorbers, varnishes and heat stabilizers in polyolefins [2–6]. Despite the literature reporting phenol alkylation catalyzed by homogeneous Bronsted acids, i.e. HClO_4 , H_3PO_4 , H_2SO_4 , HF, and Lewis acids such as BF_3 and AlCl_3 [7,8], the use of heterogeneous catalysts is favorable due to many desirable advantages.

In the past years, alkylation of phenol by tertiary butyl alcohol has been extensively studied by different types of heterogeneous materials. Till now, many gas-phase reactions which involve costly method due to high pressure and high temperature have been reported. For example, Song et al. reported a high phenol conversion by M-MCM-22 at 418 K [3]. Vinu et al. have studied the vapor-phase phenol alkylation over AlSBA-15 and reported a

phenol conversion of 86.3% at 150 °C [9]. Other related materials which have been tested by gas-phase phenol alkylation include $\text{H}_3\text{PO}_4/\text{MCM-41}$ [10], Ga-HMS-30 [7] and Al-MCM-41 [3]. It was found that a cost-effective liquid-phase phenol alkylation with *tert*-butyl alcohol over a hybrid heterogeneous catalyst is very limited in the literature.

In the current industrial advancement which emphasizes a benign environment, mesoporous molecular sieves with their distinctive textural properties (high surface area, high thermal and chemical stability) [11–13] has stimulated a tantalizing prospect of merging both organic and inorganic compounds to form new hybrid materials. The practical organic modification on silica is an excellent transformation of homogeneous catalyst into heterogeneous catalyst to overcome difficulty in product separation [9], non-reusability and corrosive nature [14].

Heterogeneous hybrid material provide pathways for generation of active sites on molecular sieves. This has opened up a wide application in catalysis and adsorption. In these few years, researchers have reported many attempts at tethering organic ligands onto mesoporous molecular sieves. Some related examples are Cyclam on SBA-15 for aerial oxidation of ethylbenzene [15], L-tryptophane on MCM-41 as a drug carrier system [16], imidazolium derivatives on MCM-41 for conversion of CO_2 to cyclic carbonate [17], Schiff base thiopene-2-carbaldehyde on MCM-41 applied in olefin epoxidation [18], 3-Mercaptomethoxysilane supported onto

* Corresponding author.

E-mail addresses: farook@usm.my, farookdr@gmail.com (F. Adam).

SBA-15, Amberlyst 15 and Nafion, MCM-41 and MCM-48 were oxidized with H_2O_2 to convert it into sulfonic acid groups. These sulfonic acid catalysts were used in the benzylation of toluene using benzyl alcohol [19,20].

In this paper, we have synthesized a sulfonic acid ligand, 3-(4-aminophenylamino)propane-1-sulfonic acid (4-NHPhSO₃H), by the reaction of 1,4-phenylene diamine and 1,3-propane sultone using a simple reflux method [21]. We report on the synthesis of new organo-inorganic hybrid hexagonal mesoporous material in which 4-NHPhSO₃H was covalently bonded to the framework of MCM-41 via direct post-synthesis method. The hybrid organo-MCM-41 was characterized by several physicochemical methods and the catalyst was used in Friedel–Craft reaction between *tert*-butanol with phenol. Various reaction conditions such as reaction time, reaction temperature, mass of catalysts and mole ratios of phenol to *tert*-butanol were studied are herein reported.

2. Experimental

2.1. The synthesis of solid acid catalyst using rice husk as the source of silica

The synthesis of silica was carried out according to literature [22,23]. Rice husk was washed with copious amount of water and rinsed with distilled water. After drying at room temperature, the rice husk was stirred with 1.0 M nitric acid at room temperature for 24 h. The rice husk was calcined in a furnace at 600 °C for 6 h to get high-purity silica. To prepare MCM-41, the required sodium silicate (Na_2SiO_3) was prepared by combining rice husk ash (6.0 g) with NaOH pellet (2.0 g) and H_2O (40.0 mL). The resulting gel mixture was heated and stirred for 2 h at 80 °C. This was labeled as solution A.

Another solution B was prepared by mixing CTAB (6.0 g) with H_2O (35.0 mL) by stirring at 80 °C until a clear solution was obtained. Solutions A and B were mixed together in a polypropylene bottle and stirred for 15 min. The mixture was then placed in an oven for crystallization at 100 °C for 24 h. The gel mixture was then cooled to room temperature. The pH of the reaction mixture was adjusted to 10.2 by drop-wise addition of 25 wt% acetic acid with vigorous stirring. The mixture was then placed in an oven for 48 h to crystallize the material. The final product was filtered, washed, dried and calcined at 550 °C in air for 10 h to obtain pure siliceous MCM-41 [23].

To modify the MCM-41, 1.0 g of MCM-41 was refluxed with 3-chloropropyltriethoxysilane (CPTES) (12.5 mmol) in toluene for 24 h [24]. The resulting solid was washed in a soxhlet apparatus with diethyl ether-dichloromethane mixture (1:1) for 12 h to remove excess reactant [25]. The resulting solid was labeled as MCM-PrCl. The yield of MCM-PrCl was 1.94 g.

The ligand, 3-(4-aminophenylamino)propane-1-sulfonic acid (4-NHPhSO₃H), was prepared by reacting 1,3-propane sultone (0.01 mol) with 1,4-phenylene diamine (0.01 mol) under reflux in acetonitrile at 80 °C. The solid product obtained was filtered by suction pump and was washed thoroughly using acetonitrile to remove the unreacted reactants. The organic ligand obtained was characterized by ¹H and ¹³C NMR spectroscopy and elemental analysis (CHN).

Immobilization of 4-NHPhSO₃H on MCM-PrCl was carried out by adding 1.0 g of MCM-PrCl (12.5 mmol), with 12.5 mmol 4-NHPhSO₃H and triethylamine (Et₃N) as deprotonating agent and refluxed in toluene at 110 °C for 24 h. The solid obtained was rinsed thoroughly with toluene, distilled water, dichloromethane and finally with acidified ethanol. The product was dried at 110 °C for 24 h and was labeled as MCM-4-NHPhSO₃H. The synthesis of the catalyst is shown in Scheme 1.

2.2. Characterization of the acid catalyst

The TEM images were obtained from a Philips CM12 instrument (Eindhoven, the Netherlands) equipped with an analyzer, Docu Version 3.2 image processing software (Munster, Germany). The SEM images were recorded using Leo Supra 50 VP FESEM, equipped with Oxford INCA 400 energy-dispersive X-ray microanalysis system (Carl-Zeiss SMT, Oberkochen, Germany; Oxford Instruments Analytical, Bucks, UK). The X-ray patterns were recorded on a Siemens Diffractometer D5000, Kristalloflex (voltage of 40 kV and current 30 mA) using Cu K α ($\lambda = 0.154$ nm) radiation. The diffraction angle was scanned in the 2 θ range, 1.5–10° for 1/2 h, at a rate of 0.050° s⁻¹. The thermogravimetric analysis (TGA) was performed using a TGA/SDTA 851^e instrument: 10.0 mg of the sample was heated from 30 to 900 °C under nitrogen flow. The elemental analysis was carried out using Perkin Elmer Series II, 2400 instrument. The ¹³C and ²⁹Si CP/MAS NMR were recorded on a Bruker AV 400 WB Solid State NMR machine, equipped with a magic angle spinning (MAS) unit. The ¹³C and ¹H liquid NMR were obtained with a Bruker Avance 111 500 MHz NMR.

2.3. Catalytic reaction

The liquid-phase alkylation experiments were carried out under argon gas in a small two-neck round-bottom flask (25 mL), equipped with a magnetic stirrer, a thermometer and a condenser. In order to prevent TBA from evaporating, ice water was used to circulate the condenser by liquid filter pump to maintain the temperature at 2 °C. In a typical run, 100 mmol of each phenol and TBA were placed in the round bottom flask containing 200 mg catalyst pre-dried for 24 h at 110 °C. The reaction mixture was stirred at 1000 rpm for 7 h. The samples of the reaction mixture were withdrawn periodically and analyzed by GC, whereby a qualitative product analysis was conducted using GC-MS. The gas chromatograph instrument was equipped with a capillary wax column (30 m length and 0.25 mm inner diameter). The temperature program was set from 40 to 46 °C at a rate of 2 °C min⁻¹, followed by 46–230 °C at a rate of 30 °C min⁻¹. Acetonitrile was used as the internal standard, which was added to the aliquots taken for GC and GC-MS analysis. The amount of acetonitrile added was 20 µL.

3. Results and discussions

3.1. The characterization of 3-(4-aminophenylamino)propane-1-sulfonic acid (4-NH₂PhSO₃H)

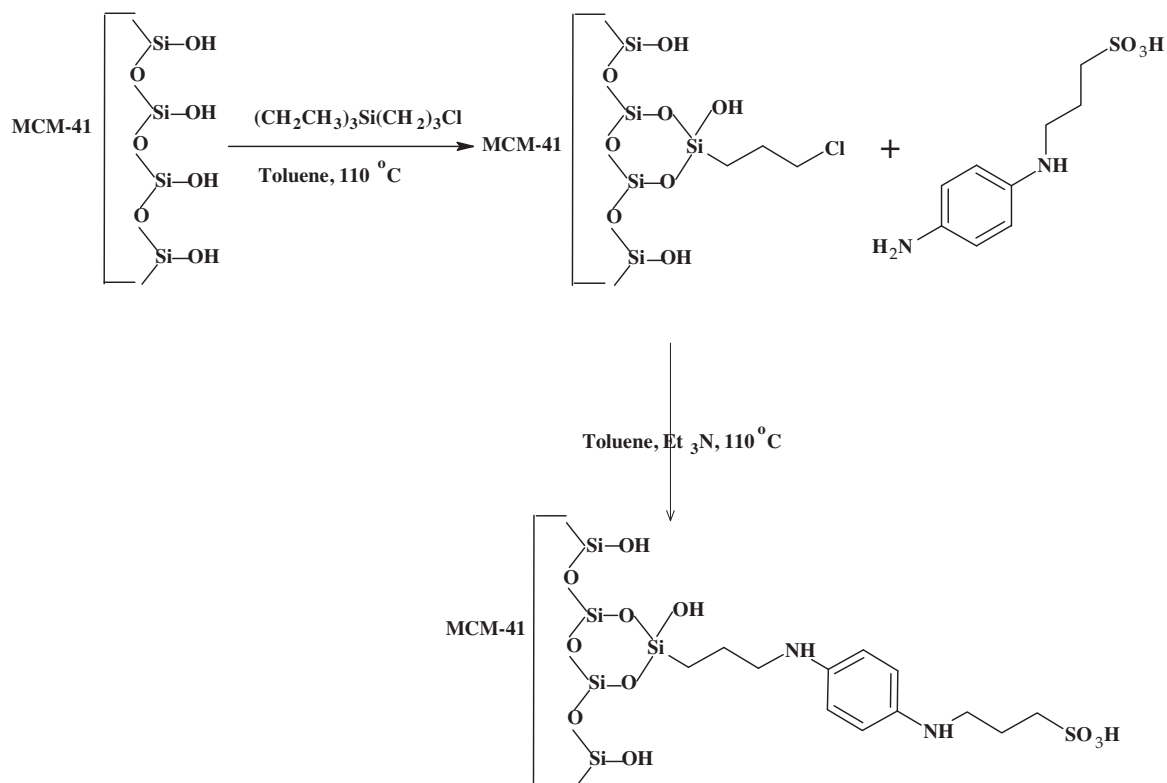
3.1.1. The ¹H and ¹³C NMR spectra of 4-NH₂PhSO₃H

The ¹H NMR spectrum (Fig. S1a) of 4-NH₂PhSO₃H confirmed the proton resonance of the –CH₂CH₂CH₂– species indicated by **Hb**, **Ha** and **Hc** at 1.88, 2.60 and 3.14 ppm. The aromatic protons, **Hd** and **He** appeared at 6.76 and 6.94 ppm, respectively. The sulfonic acid proton, **Hf** appeared at 8.56 ppm.

The ¹³C NMR spectrum (Fig. S1b) had chemical shifts for the aliphatic carbons at **Ca**, **Cb** and **Cc** at 24.33, 44.37 and 49.38 ppm, respectively. The aromatic carbons were recorded at 114.75, 119.05, 121.19 ppm for **Cd**, **Ce**, **Cf** and **Cg**, respectively. The ¹H and ¹³C NMR spectra are very consistent with the structure of 4-NH₂PhSO₃H.

3.1.2. Elemental analysis of 4-NH₂PhSO₃H

The carbon, hydrogen and nitrogen contents of 4-NH₂PhSO₃H are shown in Table 1. The deviation of the experimental value from theoretical is negligible with carbon, hydrogen and nitrogen



Scheme 1. The schematic representation of the synthesis of MCM-4-NHPhSO₃H prepared from MCM-41 derived from rice husk ash.

Table 1

The chemical analysis of 4-NH₂PhSO₃H.

	Theoretical (%)	Experimental (%)
Carbon	46.9	47.0
Hydrogen	6.1	6.0
Nitrogen	12.2	12.2

recording 46.96, 5.99 and 12.15%, respectively. The CHN analysis is consistent with the formula of 4-NH₂PhSO₃H.

3.2. The characterization of MCM-4-NHPhSO₃H

3.2.1. The X-ray diffraction pattern of MCM-4-NHPhSO₃H

Fig. 1 shows the powder X-ray diffraction (XRD) patterns of the calcined MCM-41, functionalized MCM-PrCl and MCM-4-NHPhSO₃H. The X-ray diffraction pattern of calcined MCM-41 consists of a strong reflection at $2\theta = 2.3^\circ$ assigned to the (100) reflection and three weaker reflections at higher angles corresponds to (110), (200) and (210) reflections of a hexagonal unit cell [26–28]. These reflections were maintained after the immobilization in MCM-PrCl and MCM-4-NHPhSO₃H. The shifting of reflection peaks (100), (110) and (200) to higher 2θ angle was observed. However, the mesostructure was retained after incorporating the organic groups.

3.2.2. Nitrogen sorption analysis

The nitrogen adsorption–desorption isotherms were measured at liquid nitrogen temperature for all three samples. As shown in Fig. 2, the resulting sorption isotherms were of type IV. The isotherm, which has a percolation phenomenon in the desorption branch was found to be similar to Ru-based cyclohexadiamine supported on MCM-41 reported by Soundiressane et al. [26] and chloropropyl functionalized mesoporous silica by Sujandi et al. [15]. This phenomenon could be due to the decrease in

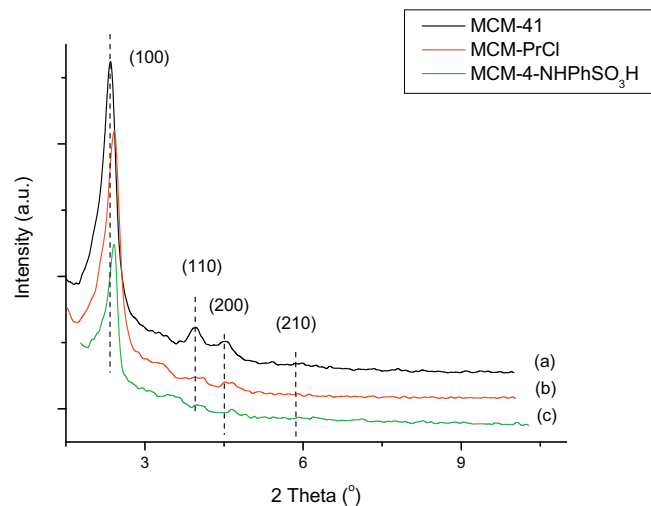


Fig. 1. The XRD patterns of (a) calcined MCM-41, (b) functionalized MCM-PrCl and (c) MCM-4-NHPhSO₃H.

mesoporosity in MCM-41, as well as the evaporation of N₂ via narrow constriction for ink-bottle cage-type mesopore [15]. The sharp step from 0.01 to 0.2 P/P₀ shows the uniform pore filling in the lattice and the capillary condensation occurs between 0.20 and 0.98 P/P₀. The specific surface areas and total pore volume were calculated by Barrett–Joyner–Halenda (BJH) method and is tabulated in Table 2. The modification resulted in the successive reduction in the respective specific surface area and pore volume from 796 m² g⁻¹ in MCM-41 to 468 m² g⁻¹ in MCM-4-NHPhSO₃H. A similar reduction in the total pore volume can also be observed. The pore diameter of MCM-41 was calculated from the desorption isotherm. The pore diameter has been reduced from 28.7 to 19.8 Å

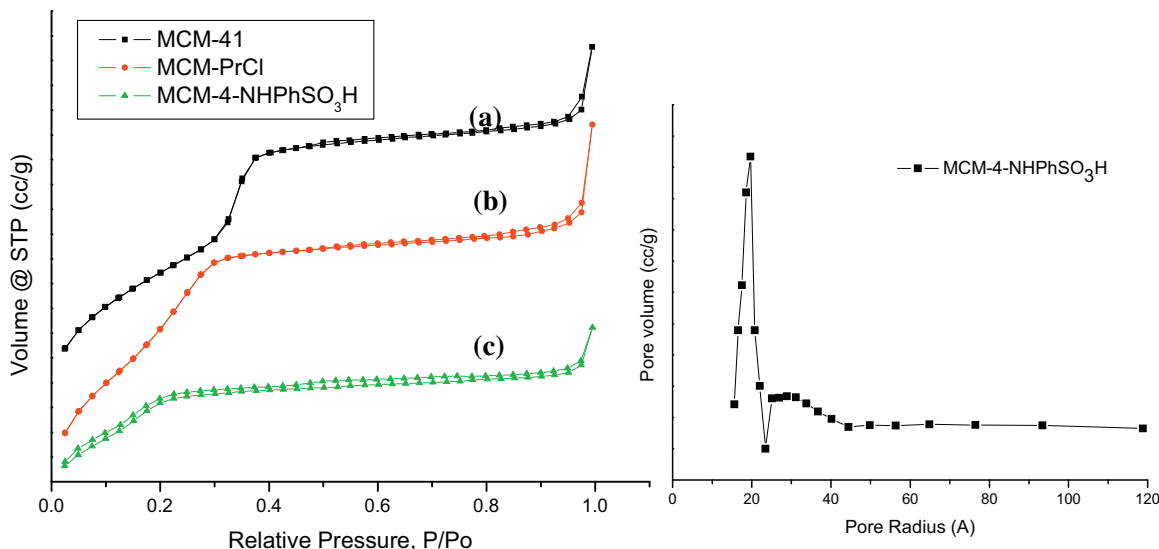


Fig. 2. N₂ adsorption and desorption isotherms at 77 K of (a) calcined MCM-41, (b) functionalized MCM-PrCl and (c) MCM-4-NHPhSO₃H and pore size distribution profiles (inset) of MCM-4-NHPhSO₃H.

Table 2
The surface properties of MCM-41 and modified samples.

Samples	d ₁₀₀ spacing (Å) ^a	Unit cell parameter, a ₀ (Å) ^b	BET surface area (m ² g ⁻¹) ^c	Pore volume, V _p (cm ³ g ⁻¹) ^c	Pore wall thickness (Å) ^b	Pore diameter, W _d (Å) ^b
MCM-41	37.9	43.8	796	0.29	15.1	28.7
MCM-PrCl	37.2	43.0	673	0.23	16.8	26.2
MCM-4-NHPhSO ₃ H	36.9	42.6	468	0.11	22.8	19.8

^a The values obtained from the XRD studies.

^b The values were calculated from the formulae [27].

^c The values obtained from N₂ sorption studies.

after every step of modification due to the accommodation of CPTES and 4-NH₂PhSO₃H inside the mesopores.

3.2.3. FT-IR spectra analysis

The FT-IR spectra of the as-synthesized MCM-41, calcined MCM-41, MCM-PrCl and MCM-4-NHPhSO₃H is shown in supplementary figure. The difference between the as-synthesized and the calcined MCM-41 can be seen from Fig. S2a and b, which shows the disappearance of the CH₂ vibration bands at 2924 and 2845 cm⁻¹ [29]. This showed the complete removal of the template, i.e. CTAB. The spectrum in Fig. S2c shows the CH₂ vibration of the propyl groups at 2928 and 2861 cm⁻¹, which proved to be due to the successful functionalization of CPTES on MCM-41. For the spectrum in Fig. S2d, the vibration band at 3228 cm⁻¹ was attributed to the secondary N-H bond which confirms the immobilization of 4-NH₂PhSO₃H. The vibration band at 3004 cm⁻¹ was assigned to the C-H aromatic system, whereas the symmetrical and asymmetrical CH₂ units were centered at 2962 and 2804 cm⁻¹. The C=C of the benzene ring was centered at 1612 and 1452 cm⁻¹, whereas the band at 1635 cm⁻¹ was attributed to O-H bending mode [30]. A strong absorption band at 1517 cm⁻¹ was due to the formation of new C-N bond between MCM-PrCl and ligand, 4-NH₂PhSO₃H by the removal of HCl. The S=O bond and –SO₃ stretching band of sulfonic group was assigned to the vibration at 1311, 1162 and 1045 cm⁻¹ [30]. All spectra show bands at 1224, 1080 and 785 cm⁻¹, which were attributed to the stretching vibrations of the mesoporous silica framework (Si-O-Si) [31].

3.2.4. Elemental analysis (CHN)

The elemental analysis of MCM-PrCl and MCM-4-NHPhSO₃H are shown in Table 3. The presence of 2.2% nitrogen and an increase in

Table 3
Elemental analysis of MCM-PrCl and MCM-4-NHPhSO₃H.

	MCM-PrCl	MCM-4-NHPhSO ₃ H
Carbon	2.7	18.0
Hydrogen	3.5	3.1
Nitrogen	0.0	2.2

carbon percentage from 2.7 to 18.0 is consistent with the immobilization of 4-NH₂PhSO₃H onto MCM-PrCl.

3.2.5. Thermogravimetric analysis (TGA)

The thermogravimetric analysis of MCM-4-NHPhSO₃H showed the weight loss before 120 °C is due to the removal of physisorbed water. The mass loss is larger than the usual physisorbed water on silica as the presence of SO₃H functional group on MCM-4-NHPhSO₃H has a tendency to adsorb water through the formation of hydrogen bonds [32]. The second mass loss which is from 146 to 509 °C was due to the decomposition of CPTES and organic groups, while the mass loss between 500 and 893 °C was due to the condensation of Si-OH groups to form a siloxane bond, losing H₂O in the process.

3.2.6. The ¹³C and ²⁹Si CP/MAS NMR analysis of MCM-4-NHPhSO₃H

The ¹³C CP MAS NMR spectrum of MCM-4-NHPhSO₃H is shown in Fig. 3a. The strong resonance at 12.27, 28.52, 49.00 and 52.75 ppm is due to the carbons of –CH₂CH₂CH₂– moiety [26,28]. The CPTES linker has three distinct carbons labeled as C10, C11 and C12, while the sulfonic acid ligand's aliphatic carbons –CH₂CH₂CH₂– are

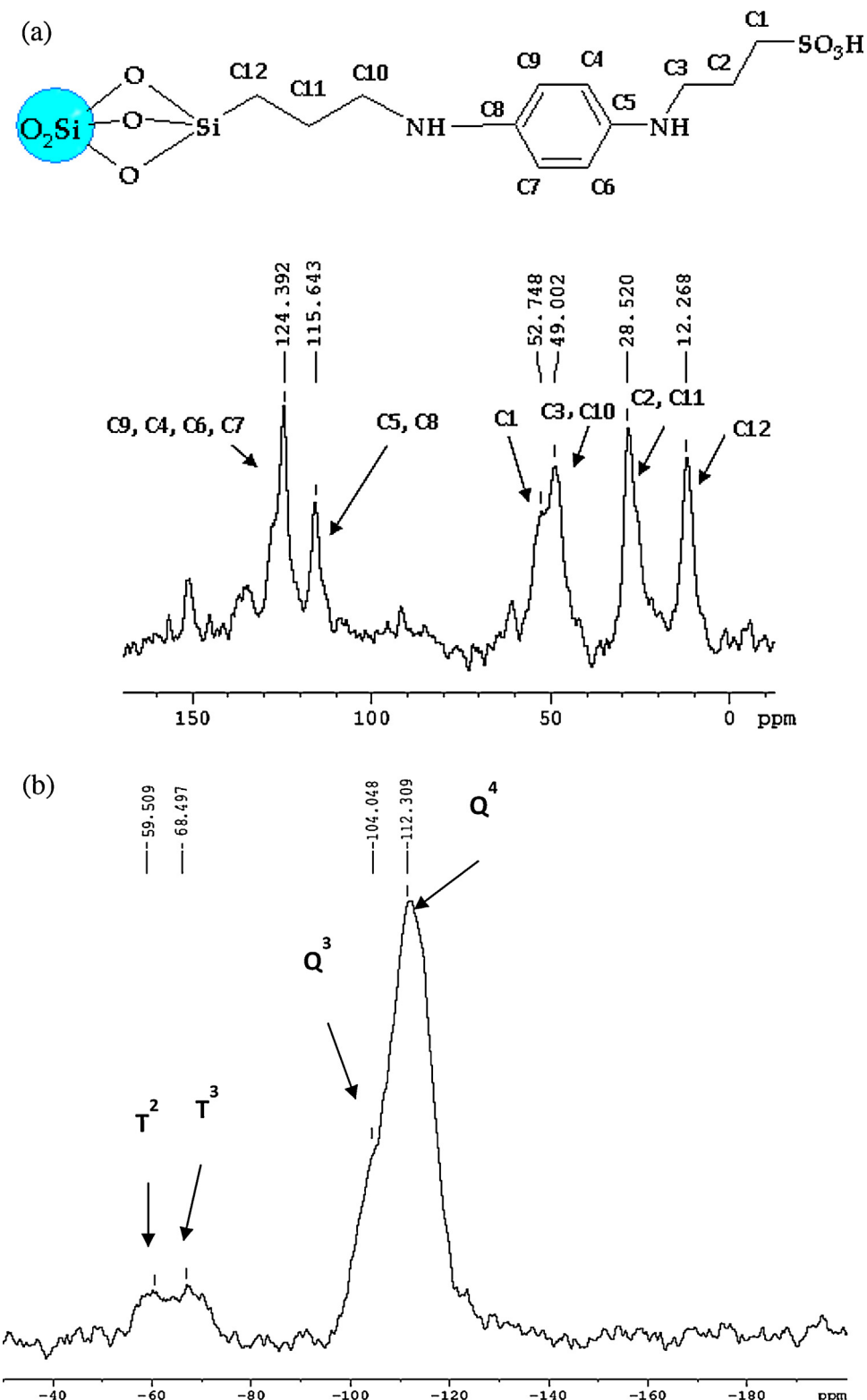


Fig. 3. The NMR spectrum of (a) the ^{13}C CP/MAS NMR and (b) ^{29}Si CP/MAS NMR of MCM-4-NHPhSO₃H.

indicated by C1, C2 and C3. The chemical shifts overlapped due to similar chemical environment. The immobilization of 4-NHPhSO₃H onto MCM-PrCl was further confirmed by the appearance of aromatic peaks at 115.64 and 124.39 ppm as indicated in Fig. 3a. The solid-state ^{13}C CP/MAS NMR spectra of MCM-4-NHPhSO₃H confirmed the presence of organic moieties as part of the silica. Fig. 3b shows the ^{29}Si CP/MAS NMR of MCM-4-NHPhSO₃H. The

distinct resonances can be clearly observed for the siloxane network with organic fragments covalently bonded to silica: the chemical shift at -104.05 ppm for the Q³ silicon atom of the silica solid, a chemical shift at -112.31 ppm for the Q⁴ silicon atom in the silica solid [Qⁿ = Si(OSi)ⁿ(OH)⁴⁻ⁿ, n = 2–4]; the T³ and T² signals of the organosilicon atoms are seen at -68.50 and -59.51 ppm, respectively [T^m = RSi(OSi)^m(OH)^{3-m}, m = 1–3] [33].

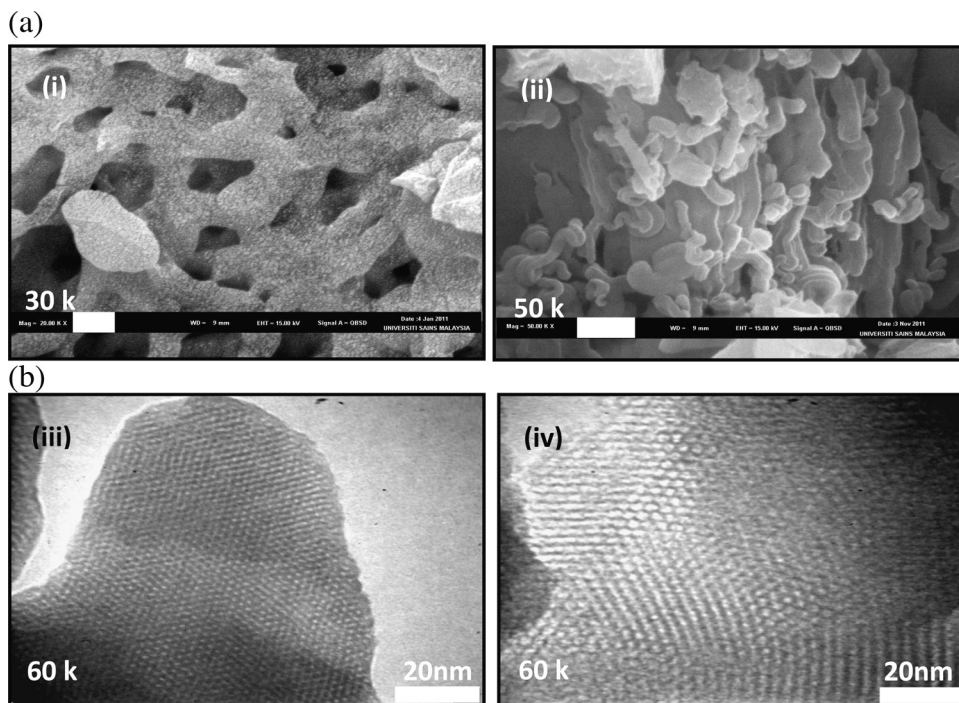


Fig. 4. The scanning electron micrographs: (a) The SEM morphology of (i) MCM-PrCl and (ii) MCM-4-NHPhSO₃H and (b) the TEM image of (iii) MCM-PrCl and (iv) MCM-4-NHPhSO₃H.

3.2.7. The transmission electron microscopy (TEM) and scanning electron microscopy (SEM)

Fig. 4a(i) and **a(ii)** show the surface morphology of MCM-PrCl and MCM-4-NHPhSO₃H with the presence of large orifices and overlapping cylindrical worm-like structure at 30 k and 50 k magnification. The TEM images of MCM-PrCl and MCM-4-NHPhSO₃H show the well structured honey-comb design after immobilization of the organic moiety as shown in **Fig. 4b(iii)** and **(iv)**.

3.3. Catalytic alkylation

The Friedel-Craft alkylation of phenol by *t*-butyl alcohol (**Scheme 2**) was carried out over MCM-4-NHPhSO₃H from 100 to 120 °C, with various catalyst amount and molar ratio. The obtained products were 2-(*tert*-butyl)phenol (2-TBP), 4-(*tert*-butyl)phenol (4-TBP) and some minor *tert*-butylphenol ether (TBPE) and isobutene (IBE). The reaction scheme may be depicted as follows.

3.3.1. Effect of time on TBA conversion

Fig. 5 shows the relative activity and product selectivity of MCM-4-NHPhSO₃H as a function of time for alkylation of phenol by TBA at 120 °C and 1:1 molar ratio of phenol to TBA using 20 mg of catalyst. Initially, the conversion of TBA was 25.0% in 1 h, with the main product selective to TBPE and then it decreased with time as the selectivity towards 2-TBP and 4-TBP increased. The conversion of TBA increased with reaction time until it reached an equilibrium level at 7 h. The final conversion at 7 h is 96.0% with the selectivity towards monoalkylated products, 2-TBP (56.0%) and 4-TBP (37.0%).

3.3.2. Effect of reaction temperature

The effect of reaction temperature on the conversion of TBA was performed in the range of 100–120 °C as shown in **Fig. 6**. At a lower temperature of 100 °C, the conversion of TBA was only 28.0% with a very high selectivity of 95.0% to TBPE. This could be due to the likelihood of *o*-alkylation occurring at the lower activation energy, which prompted the high TBPE selectivity [10,34]. As the reaction temperature increased to 120 °C, 96.0% conversion of TBA was obtained,

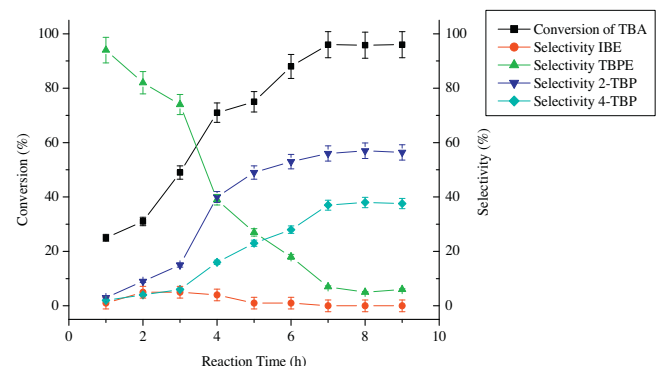
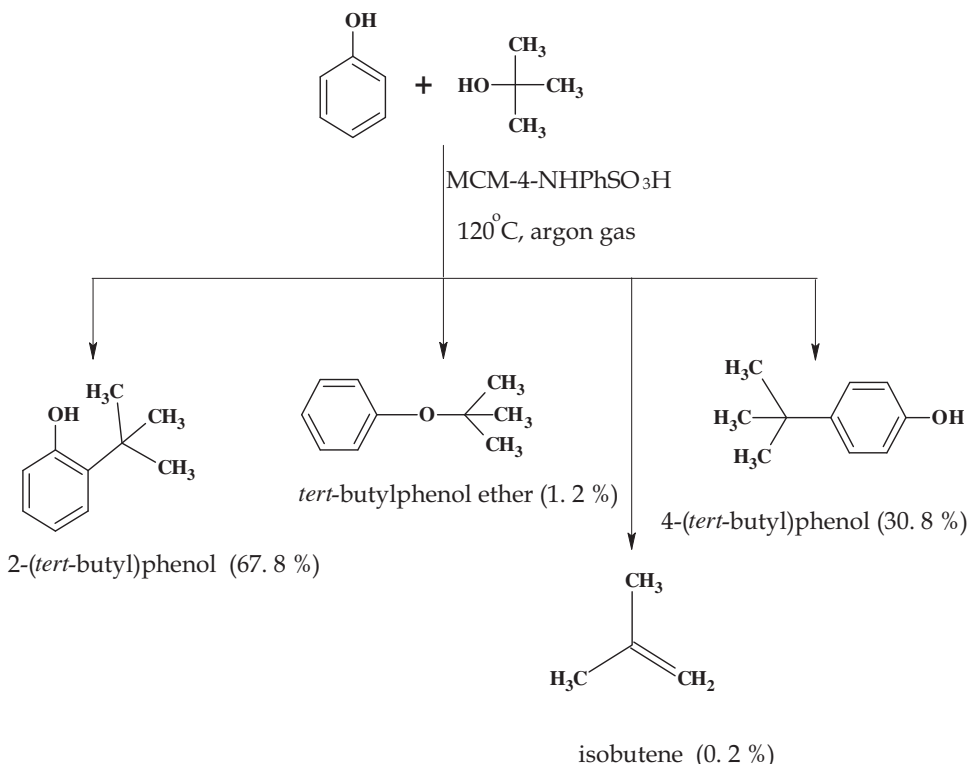


Fig. 5. The effect of reaction time on *t*-butylation of phenol by MCM-4-NHPhSO₃H. Reaction conditions: molar ratio of TBA (100 mmol):phenol = 1:1, catalyst amount = 200 mg, reaction temperature 120 °C, run time = 9 h.

with 56.0 and 37.0% selectivity to 2-TBP and 4-TBP, respectively. Zhang et al. [5] reported only 68.0% conversion of TBA, with 26.0% selectivity to 2-TBP. This shows that the organo hybrid catalyst in this study performs better than the HY zeolite reported by Zhang et al.

3.3.3. Effect of catalyst amount

Fig. 7 shows the effect of catalyst amount on TBA conversion studied within the range of 30–200 mg. All the different masses of catalysts used gave approximately 98.0% conversion when the reactions were carried out for 7 h. However, in order for a meaningful comparison, the reaction time of 4 h was selected. The increase in amount of catalyst from 30 to 50 mg had significantly increased the conversion of TBA to 98.4% in 4 h with a selectivity of 62.0 and 33.0% for 2-TBP and 4-TBP, respectively. This result was an improvement from the previous work by Adam et al. [30] which reported a 95.0% TBA conversion in 9 h instead of 4 h reported herein. When the catalyst amount was increased beyond 50 mg, gradual decrease in overall conversion could be observed, with increasing selectivity



Scheme 2. The reaction scheme for *tert*-butylation of phenol.

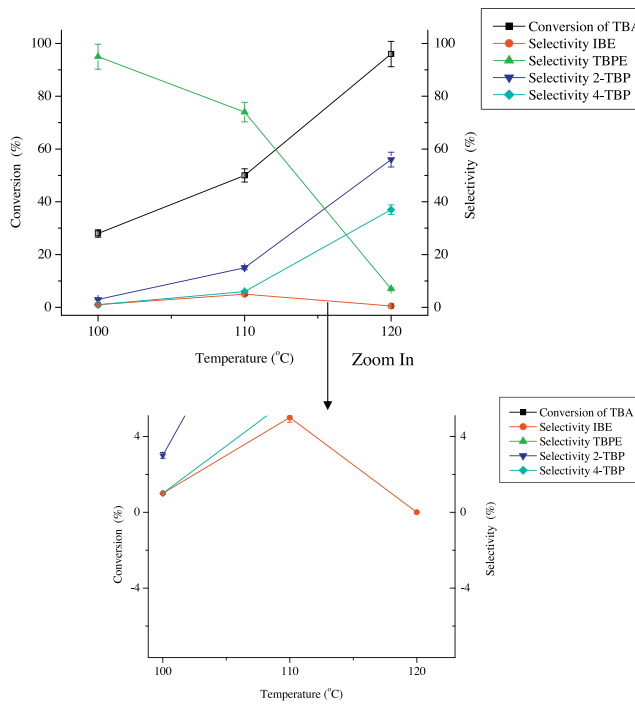


Fig. 6. The effect of reaction temperature on *t*-butylation of phenol by MCM-4-NHPhSO₃H. Reaction conditions: molar ratio of phenol (100 mmol):TBA = 1:1, mass of catalyst = 20 mg, 7 h.

to TBPE from 4.0 to 41.0%. The selectivity to the main products of mono-alkylated 2-TBP and 4-TBP was found to gradually decrease with increasing catalyst mass. This could be explained by the large amount of catalyst which gives rise to agglomeration and cause pore blocking of the active sites when the catalyst amount was increased above 50 mg.

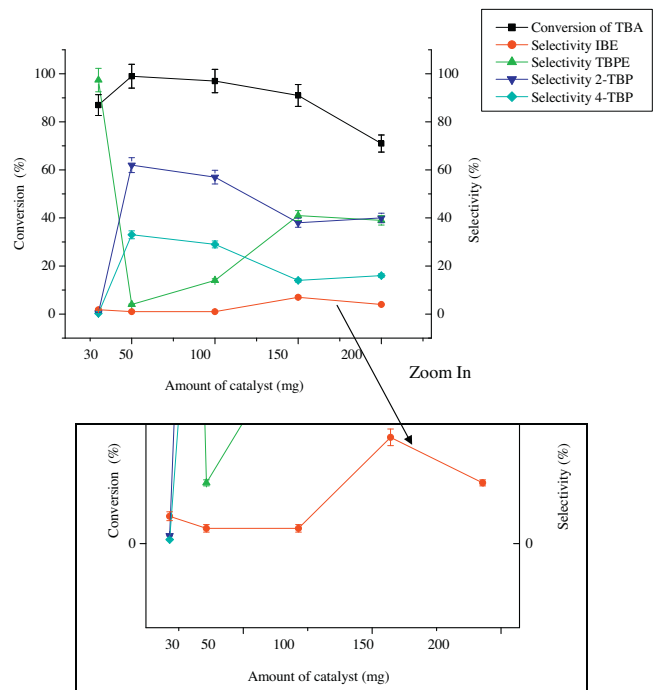


Fig. 7. The effect of catalyst amount on *t*-butylation of phenol by MCM-4-NHPhSO₃H. Reaction conditions: molar ratio of phenol (100 mmol):TBA = 1:1, 120 °C, 4 h.

3.3.4. Effect of mole ratio on TBA conversion

The effect of reactant mole ratio of TBA to phenol was conducted in the range of 1:1, 1:2 and 1:3. From Fig. 8, it can be observed that as the TBA:phenol feed mole ratio increased from 1:1 to 1:3, the optimum mole ratio of 1:2 of TBA to phenol was found to have the highest selectivity for 2-TBP (67.8%). A total of 99.5% conversion of

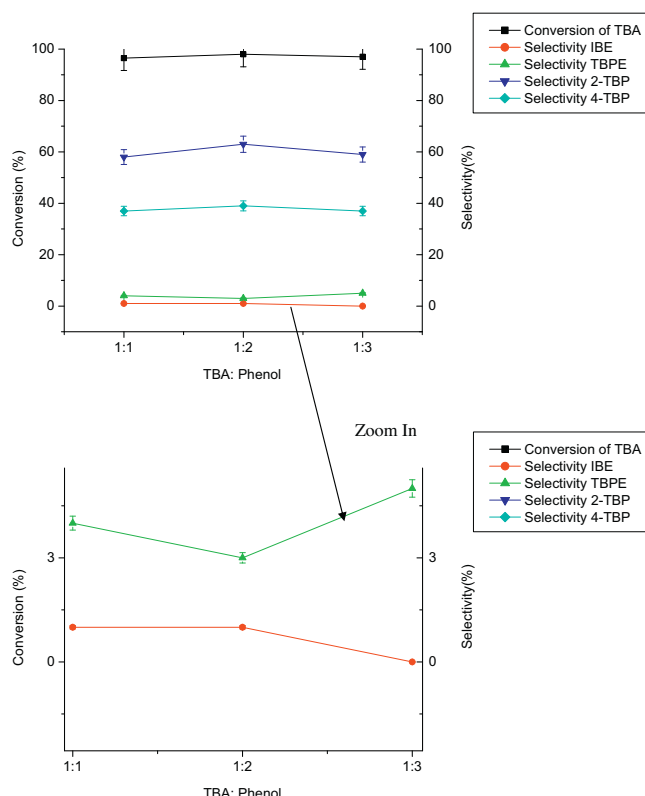


Fig. 8. The effect of reactant mole ratio on *t*-butylation of phenol by MCM-4-NHPhSO₃H. Reaction conditions: mass of catalyst = 50 mg, 120 °C, 4 h.

TBA was recorded in a short 4 h reaction time. The higher affinity of phenol adsorbing on the active sites allows the primary generation of carbenium ion to react readily with sufficient phenol adsorbed in close proximity [35]. Furthermore, the higher ratio of phenol to TBA is able to prevent formation of dialkylated products [35]. The reported catalytic activity was two times faster from the work by Adam et al. which reported a 95.0% conversion of TBA within a longer reaction time of 9 h [30].

3.3.5. Reusability studies on the catalyst

In order to study the recoverability and recyclability of MCM-4-NHPhSO₃H, this organo-hybrid catalyst was regenerated by simple washing with dichloromethane, acidified ethanol and dried at 110 °C for 24 h. Fig. 9 shows only a slight decrease in the catalytic activity after several reuse under the optimum conditions of 120 °C, with 50 mg of catalyst and 1:2 mole ratio of TBA:phenol for 4 h. This could be due to the loss of active catalytic sites after several consecutive reused. Some of the organic ligands anchored on the external surface and accessible pores of MCM-41 could be washed away by the solvents. This can be further correlated with the XRD analysis of the reused MCM-4-NHPhSO₃H. The used catalyst was characterized once again using the XRD and TEM analyses. The image in Fig. S3 shows that the catalyst's morphology was not altered upon being used as a catalyst.

3.3.6. Conversion of TBA over MCM-41 and MCM-PrCl (as control)

The activity of MCM-41 and MCM-PrCl, both as controls, were investigated using the optimum conditions. There was no reaction detected when MCM-41 was used as the catalyst in the *tert*-butylation of phenol. The use of MCM-PrCl as catalyst resulted in only 15.4% conversion of TBA with the selectivity towards the minor products of IBE (18.2%) and TBPE (81.8%). The desired mono-alkylated products of 2-TBP and 4-TBP were not obtained.

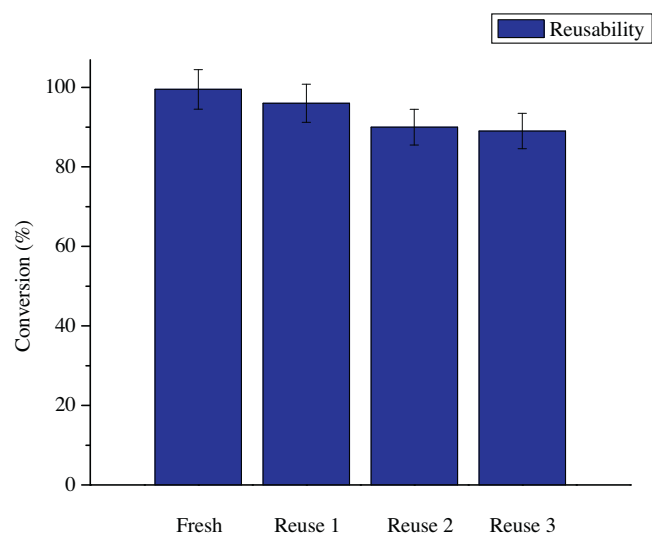


Fig. 9. The reusability of MCM-4-NHPhSO₃H in the *t*-butylation of phenol. Reaction conditions: molar ratio of phenol (100 mmol):TBA = 2:1, mass of catalyst = 50 mg, 120 °C, 4 h.

This shows that the catalytic activity depends on the presence of the sulfonic acid group on the catalyst surface. It should be highlighted here that if one desires to obtain TBPE in high yield, then MCM-PrCl could be used as the catalyst. It is believed that this reaction is worthwhile investigating in the future, despite the fact the conversion was only 15.4%.

4. Conclusions

A novel organo-inorganic hybrid material was successfully synthesized via a simple post-synthesis method. The organic species bearing the sulfonic acid group was able to tether onto the MCM-41 mesoporous silica and maintained the honey-comb structure of the original MCM-41. The catalyst was tested in the solvent-free liquid-phase *tert*-butylation of phenol and gave a high 99.5% TBA conversion in 4 h with good selectivity of 67.8% 2-TBP and 30.8% 4-TBP. The catalyst was selective to only mono-alkylated products.

Acknowledgements

The authors would like to thank Universiti Sains Malaysia for the Postgraduate Research Grant Scheme (PRGS) (1001/PKIMIA/844073 and 1001/PKIMIA/811092) and RU research grant (No. PKIMIA/814019) which partly supported this work. C.W.K. would also like to thank the National Science Fellowship (NSF) of Malaysia for the scholarship provided.

Appendix A. Supplementary data

Supplementary data associated with this article can be found, in the online version, at <http://dx.doi.org/10.1016/j.apcata.2014.09.047>.

References

- [1] M.F. Matloubi, M. Akhlaghil, L. Hojabril, M.G. Dekamin, Trans. C: Chem. Eng. 16 (2009) 81–88.
- [2] E. Modrogañ, M.H. Valkenberg, W.F. Hoelderich, J. Catal. 261 (2009) 177–187.
- [3] K. Song, J. Guan, S. Wu, Y. Yang, B. Liu, Q. Kan, Catal. Lett. 126 (2008) 333–340.
- [4] P. Elavarasan, K. Kondamudi, S. Upadhyayula, Chem. Eng. J. 166 (2011) 340–347.
- [5] K. Zhang, H. Zhang, G. Xu, S. Xiang, D. Xu, S. Liu, H. Li, Appl. Catal. A: Gen. 207 (2001) 183–190.
- [6] H.-Y. Shen, Z.M.A. Judeh, C.B. Ching, Tetrahedron Lett. 44 (2003) 981–983.

- [7] K. Bachari, A. Touileb, M. Touati, O. Cherifi, *J. Mol. Catal. A: Chem.* 294 (2008) 61–67.
- [8] H.-Y. Shen, Z.M.A. Judeh, C.B. Ching, Q.-H. Xia, *J. Mol. Catal. A: Chem.* 212 (2004) 301–308.
- [9] A. Vinu, B.M. Devassy, S.B. Halligudi, W. Böhlmann, M. Hartmann, *Appl. Catal. A: Gen.* 281 (2005) 207–213.
- [10] M. Ghiaci, B. Aghabarari, *Chin. J. Catal.* 31 (2010) 759–764.
- [11] A. Sakthivel, W. Sun, G.S. Raudaschl, A.S.T. Chiang, M. Hanzlik, F.E. Kuhn, *Catal. Commun.* 7 (2006) 302–307.
- [12] E.-P. Ng, H. Nur, K.-L. Wong, M.N.M. Muhib, H. Hamdan, *Appl. Catal. A* 323 (2007) 58–65.
- [13] L. Yan, L. Jun, *Microp. Mesop. Mater.* 86 (2005) 23–30.
- [14] E. Dumitri, D. Meloni, R. Monaci, V. Solinas, C.R. Chimie (2005) 443–456.
- [15] E.A. Sujandi, D.-S. Han Prasetynanto, S.-C. Lee, S.-E. Park, *Catal. Today* 141 (2009) 374–377.
- [16] Z. Li, K. Su, B. Cheng, Y. Deng, *J. Colloid Interf. Sci.* 342 (2010) 607–613.
- [17] S. Udaykumar, M.-K. Lee, H.-L. Shim, S.-W. Park, D.-W. Park, *Catal. Commun.* 10 (2009) 659–664.
- [18] S. Tangestaninejad, M. Moghadam, V. Mirkhani, I.M. Baltork, K. Ghani, *Catal. Commun.* 10 (2009) 853–858.
- [19] P.F. Siril, N.R. Shiju, D.R. Brown, K. Wilson, *Appl. Catal. A: Gen.* 364 (2009) 95–100.
- [20] M. Bandyopadhyay, N.R. Shiju, D.R. Brown, *Catal. Commun.* 11 (2010) 660–664.
- [21] W.F. Erman, H.C. Kretschmar, *Syntheses and Facile Cleavage of Five-Membered Ring Sultams*, Vol. 26, Procter & Gamble Co, Miami Valley Laboratories, 1961.
- [22] F. Adam, H. Osman, K.M. Hello, *J. Colloid Interf. Sci.* 331 (2009) 143–147.
- [23] E.-P. Ng, H. Nur, K.-L. Wong, M.N.M. Muhib, H. Hamdan, *Appl. Catal. B* 137 (2006) 1135.
- [24] G. Jayamurugan, C.P. Umesh, N. Jayaraman, *J. Mol. Catal. A* 307 (2009) 142–148.
- [25] D. Brunel, *Microp. Mesop. Mater.* 27 (2009) 329–344.
- [26] T. Soundiressane, S. Selvakumar, S. Menage, O. Hamelin, M. Fontecave, A.P. Singh, *J. Mol. Catal. A: Chem.* 270 (2007) 132–143.
- [27] M. Masteri-Farahani, *J. Mol. Catal. A: Chem.* 316 (2010) 45–51.
- [28] C. Venkatesan, A.P. Singh, *J. Catal.* 227 (2004) 148–163.
- [29] H.R. Li, J. Lin, L.S. Fu, J.F. Guo, Q.G. Meng, F.Y. Liu, H.J. Zhang, *Microp. Mesop. Mater.* 55 (2002) 103–107.
- [30] F. Adam, K.M. Hello, T.H. Ali, *Appl. Catal. A* 399 (2011) 42–49.
- [31] Y. Li, B. Yan, *Sol. State Sci.* 11 (2009) 994–1000.
- [32] J. Yang, Q. Yang, G. Wang, Z. Feng, J. Liu, *J. Mol. Catal. A* 256 (2006) 122–129.
- [33] X. Wang, G. Wu, J. Li, N. Zhao, W. Wei, Y. Sun, *J. Mol. Catal. A: Chem.* 276 (2007) 86–94.
- [34] E. Dumitriu, V. Hulea, *J. Catal.* 218 (2003) 249–257.
- [35] K. Ojha, N.C. Pradhan, A.N. Samanta, *Chem. Eng. J.* 112 (2005) 109–115.